Fast emergency control strategy calculation based on dynamic equivalence and integral sensitivity

Yi-fan GAO, Jian-quan WANG[†‡], Tan-nan XIAO, Dao-zhuo JIANG

College of Electrical Engineering, Zhejiang University, Hangzhou 310027, China

[†]E-mail: wangjq@zju.edu.cn

Abstract: To simplify the transient stability analysis of a large-scale power system and realize real-time emergency control, a fast transient stability simulation algorithm based on real-time dynamic equivalence is proposed. Generator models are grouped and aggregated according to a fast numerical integration. A fast calculation method of the admittance matrix is then proposed to calculate the parameters of an equivalent system, and numerical integration is performed using the obtained equivalent system. Then, based on integral sensitivity, a new fast emergency control strategy is proposed for the equivalent system. The final emergency control strategy is obtained by mapping the control strategy for the equivalent system back to the original system. The results of a simulation on an East China Power System that includes 496 generators and 5075 buses show that the suggested algorithm can output an accurate transient stability simulation result and form an effective emergency control strategy. The proposed algorithm is much faster than the existing solutions and has the potential to be used for online pre-decision.

1 Introduction

Continuous expansion of power systems makes the power system operation environment more complex (Tian et al., 2016). Emergency control, including generator tripping, load shedding, and controlled system separation, is essential to ensure stable operation and a continuous power supply, even with large disturbances. As is well known, an effective emergency controller should be initiated very quickly in a few hundred milliseconds after a fault occurs (Li et al., 2002). Because a modern power system is a high-dimensional, nonlinear, and large dynamic system, traditional emergency controls are often not fast enough for real-time applications. Therefore, a practical algorithm that can rapidly and accurately arrive

at a control strategy is needed.

There are three main methods for achieving transient stability constrained emergency control. The first is a direct method based on the transient energy function (Xue, 1993; Song and Kezunovic, 2004; Chiang, 2011). The second is an intelligent algorithm (Nakawiro and Erlich, 2009). The third translates the original problem into an optimal control problem that accounts for the constraints of differential-algebraic equations (Jiang et al., 2014). Song and Kezunovic (2004) introduced a stability control scheme based on a Lyapunov direct method, the potential energy boundary surface method, and the analytical sensitivity of the transient energy margin. A fast and accurate control goal can be obtained from this control scheme; however, the results of the scheme may have reliability issues. Chiang (2011) established an emergency control strategy using a boundary of stability method based on controlling an unstable equilibrium point. The calculation results may be conservative because misjudgment of the unstable model

---

introduces errors. Xue (1993) first proposed online pre-decision and real-time matching, and made full use of computer parallel processing and the latest achievement of extended equal area criteria (EEAC), which is a big step forward for emergency control. However, although their probability is very small, some major accidents might not be predicted completely and controlled effectively. Nakawiro and Erlich (2009) proposed an ant colony optimization based algorithm to solve the optimal load-shedding problem. The method is intuitive and easily obtains a feasible solution, but requires too much calculation time; therefore, it is not suitable for real-time applications. Jiang et al. (2014) guaranteed first-swing transient stability using a parallel reduced-space interior point method with orthogonal collocation to solve the first-swing stability constrained emergency control problems with excellent computational efficiency.

In this study, a new fast emergency control strategy algorithm is proposed, using a new transient stability simulation algorithm. The generator equivalence is calculated using model aggregation in a static extended equal area criterion (SEEAC), which simplifies the complex mathematical process and noise filtering steps compared with the traditional equivalence estimate. Also, our emergency control strategy, which is based on integral sensitivity, quickly finds the optimization direction for control variables. Compared with the existing methods mentioned above, the basic concept of EEAC generator grouping is introduced in this study. Unlike the method of EEAC generator grouping, the generators are grouped according to the rotor angle movement curves for a period of time. That is to say, if the rotor angles of all the generators appear in *n* kinds of movement trends, generators are grouped into *n* groups; generators do not have to be grouped into two groups, which preserves the characteristics of the original system. The algorithm in this study approaches emergency control as an optimal control problem. Instead of performing stability analysis using an equal area criterion for a one-machine infinite bus system, the method performs stability analysis using numerical integration and obtains the emergency control strategy using integral sensitivity on a multi-machine equivalent system.

2 Fast transient stability simulation algorithm based on real-time dynamic equivalence

Aiming at real-time analysis and control, in this section, we propose a fast transient stability simulation algorithm using the idea of dynamic equivalence. A fast numerical integration is performed using the original system, and the generators are classified in several groups according to their rotor angle curves, preserving the characteristics of the original system. Generators are model aggregated using the concept of center of inertia (COI) and the model aggregation method in an EEAC (Xue et al., 1988a, 1988b, 1992, 1993; Xue and Pavella, 1989; Euxibie et al., 1992). A new admittance matrix fast calculation method is also proposed, which substantially simplifies calculation and speeds up the algorithm.

2.1 Generator grouping

First, time t_e is set based on experience after all faults and operations are completed. Before t_e, if the rotor angle curves of two generators are close, then the generators are grouped together. The variance of rotor angles at every integration step before t_e is used as a standard for generator grouping. Assuming that ε is the threshold of variance, two generators are grouped if the following conditions are satisfied:

$$S_{ij}^2 = \frac{1}{N_E - 1} \sum_{k=1}^{N_E} \left(\Delta\delta_{kij} - \overline{\Delta\delta_{ij}} \right)^2 < \varepsilon, \qquad (1)$$

$$\Delta\delta_{kij} = \delta_{ki} - \delta_{kj}, \ k = 1, 2, \ldots, N_E, \qquad (2)$$

$$\overline{\Delta\delta_{ij}} = \frac{1}{N_E} \sum_{k=1}^{N_E} \Delta\delta_{kij}, \qquad (3)$$

where N_E represents the total number of numerical integration steps before time t_e, δ_{ki} and δ_{kj} represent the power angles of generators i and j at time step k respectively, $\overline{\Delta\delta_{ij}}$ represents the average value of the power angle difference between generators i and j in time interval $(0, t_e)$, and S_{ij}^2 represents the variance value of the power angle difference between generators i and j in time interval $(0, t_e)$.

2.2 Generator equivalence

Generators in the same group should be model aggregated, and all parameters of the equivalent

generators should be obtained before calculation using the equivalent system. COI is used to describe the stability performance of the equivalent generators (Yuan et al., 2003).

For group i, which contains ng_i generators with rotor angle δ_{i_p} and inertia constant M_{i_p}, the position of the COI is defined as

$$\delta_{\mathrm{COI}i} = \frac{1}{M_{\mathrm{COI}i}} \sum_{p=1}^{\mathrm{ng}_i} M_{i_p} \delta_{i_p}, \tag{4}$$

$$M_{\mathrm{COI}i} = \sum_{p=1}^{\mathrm{ng}_i} M_{i_p}. \tag{5}$$

If an equivalent speed and an equivalent angle are found for each group, the values of the machine parameters can be deduced. The stator winding voltage equations and stator winding flux linkage equations are given as (Wang et al., 2008)

$$\begin{cases} V_{\mathrm{d}} = p\psi_{\mathrm{d}} - \omega\psi_{\mathrm{q}} - r_a I_{\mathrm{d}}, \\ V_{\mathrm{q}} = p\psi_{\mathrm{q}} + \omega\psi_{\mathrm{d}} - r_a I_{\mathrm{q}}, \end{cases} \tag{6}$$

$$\begin{cases} \psi_{\mathrm{d}} = E_{\mathrm{q}}'' - X_{\mathrm{d}}'' I_{\mathrm{d}}, \\ \psi_{\mathrm{q}} = -E_{\mathrm{d}}'' - X_{\mathrm{q}}'' I_{\mathrm{q}}. \end{cases} \tag{7}$$

Under the classical model, E_{q}'' and E_{d}'' are replaced by E' and 0 respectively, and X_{q}'' and X_{d}'' are replaced by X_{q} and X_{d}' respectively. If $p\psi_{\mathrm{d}}=p\psi_{\mathrm{q}}=0$, $\omega=1$ p.u., and $r_a=0$, we substitute Eq. (7) into Eq. (6) to obtain the following stator voltage equation:

$$\begin{cases} V_{\mathrm{d}} = X_{\mathrm{q}} I_{\mathrm{q}}, \\ V_{\mathrm{q}} = E' - X_{\mathrm{d}}' I_{\mathrm{d}}. \end{cases} \tag{8}$$

So, if the stator winding current and voltage are calculated, X_{q} and X_{d}' can be directly deduced. However, as will be described in Section 2.3, the stator winding voltage can be calculated only when the generator parameters are given. The parameter calculation for each equivalent generator is the same as that in the method of SEEAC (Xue and Zhang, 1990):

$$X_{\mathrm{q}i} = \sum_{p=1}^{\mathrm{ng}_i} (X_{\mathrm{q}i_p})^{-1}, \tag{9}$$

$$X_{\mathrm{d}i}' = \sum_{p=1}^{\mathrm{ng}_i} (X_{\mathrm{d}i_p}')^{-1}, \tag{10}$$

where $X_{\mathrm{d}i}'$ and $X_{\mathrm{q}i}$ represent the direct-axis transient reactance and the quadrature-axis synchronous reactance of the equivalent generator in group i respectively, $X_{\mathrm{d}i_p}'$ and $X_{\mathrm{q}i_p}$ represent the direct-axis transient reactance and the quadrature-axis synchronous reactance of generator p respectively, which belongs to the equivalent generator i.

2.3 Calculation of the equivalent system admittance matrix

In this subsection, we propose a method to calculate the admittance matrix of the equivalent system. Before numerical integration is performed on the equivalent system, the structure parameters of the equivalent system should be calculated. If the original system is divided into m groups before time t_{e}, the equivalent system consists of m generators that are fully connected, and the admittance matrix for the equivalent system is an m-dimensional full matrix that contains $m \times m$ unknown elements. Because the node injecting current and the node voltage meet the relationship of $\boldsymbol{YV}=\boldsymbol{I}$ at every integration time step, the admittance matrix can be identified if the adequate node injecting currents and node voltages are known. Because an information set can be obtained that includes node injecting currents and node voltages for all the m equivalent generators at one time step, to calculate the $m \times m$ unknown quantities, m information sets should be obtained in total. The detailed method is presented as follows. Assuming that t_{c} ($t_{\mathrm{c}}<t_{\mathrm{e}}$) is the time when all emergency controls are completed, m steps of numerical integration values after t_{c} could be used to calculate the admittance matrix. The injecting currents of all generators at time steps $t_{\mathrm{e}}-(m-1)\Delta t$, $t_{\mathrm{e}}-(m-2)\Delta t$, …, t_{e} can be obtained from numerical integration, containing m total time steps. The injecting currents I_{xi} and I_{yi} of an equivalent generator i are equal to the sum of all generator injecting currents in group i. The bus voltages V_{xi} and V_{yi} of the

equivalent generator i at every time step can be calculated as

$$\begin{bmatrix} I_{xi} \\ I_{yi} \end{bmatrix} = \begin{bmatrix} g_{xi} & b_{xi} \\ b_{yi} & g_{yi} \end{bmatrix} \begin{bmatrix} 0 \\ E_i' \end{bmatrix} - \begin{bmatrix} G_{xi} & B_{xi} \\ B_{yi} & G_{yi} \end{bmatrix} \begin{bmatrix} V_{xi} \\ V_{yi} \end{bmatrix}. \quad (11)$$

After the generator voltages and injecting currents of all m steps are obtained, the admittance matrix is calculated as

$$\mathbf{Y} = \begin{bmatrix} I_1[t_e - (m-1)\Delta t] & I_1[t_e - (m-2)\Delta t] & \cdots & I_1 t_e \\ I_2[t_e - (m-1)\Delta t] & I_2[t_e - (m-2)\Delta t] & \cdots & I_2 t_e \\ \vdots & \vdots & & \vdots \\ I_m[t_e - (m-1)\Delta t] & I_m[t_e - (m-2)\Delta t] & \cdots & I_m t_e \end{bmatrix}$$
$$\cdot \begin{bmatrix} V_1[t_e - (m-1)\Delta t] & V_1[t_e - (m-2)\Delta t] & \cdots & V_1 t_e \\ V_2[t_e - (m-1)\Delta t] & V_2[t_e - (m-2)\Delta t] & \cdots & V_2 t_e \\ \vdots & \vdots & & \vdots \\ V_m[t_e - (m-1)\Delta t] & V_m[t_e - (m-2)\Delta t] & \cdots & V_m t_e \end{bmatrix}^{-1}.$$
$$(12)$$

Although the admittances of the pre-, during-, and post-fault are generally different, the calculation of admittance is performed after all faults and operations are completed. So, the admittance matrix will not change after t_c. Although the admittance matrix of the equivalent system is no longer sparse, the calculation requires very little time, because the dimension of the matrix is small. On the other hand, the majority of numerical integration is performed using the equivalent system, ensuring that the algorithm saves a lot of calculation time. The simplified system is shown in Fig. 1. The system contains only m active nodes, which are fully connected. The constant impedance loads have already been incorporated into the admittance matrix. Because the injecting current is used to calculate the admittance matrix rather than the dummy injecting current, the dummy admittance of the equivalent generators still has to be incorporated into the admittance matrix, which will be detailed in Section 3.2.

2.4 Calculation procedure

Fig. 2 shows the order of timing points and different calculation processes. Note that calculation using the original system until t_e is done only to obtain
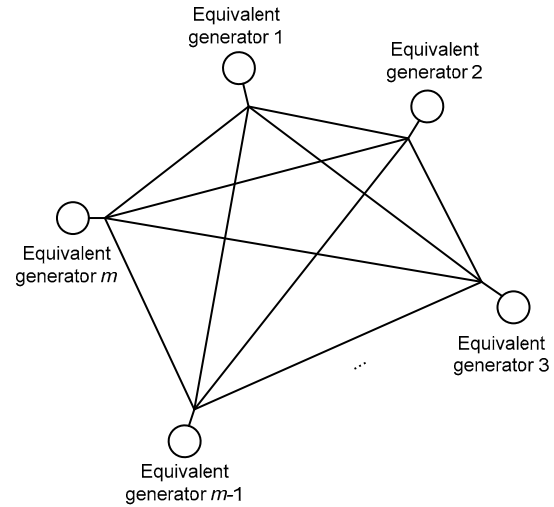

Fig. 1　Network structure of the equivalent system

information for generator grouping and admittance matrix calculation. If the transient stability algorithm is applied to emergency control, which will be explained in detail in Section 5, then calculation using the equivalent system should start from t_c; thus, the gradient of control variables can be obtained. In this part, the calculation using the equivalent system could start from t_e.

The calculation procedure of the fast transient stability simulation algorithm based on real-time dynamic equivalence (Algorithm 1) is summarized below:

1. Perform fast numerical integration using the original system until time t_e.

2. Group the generators in box 1 as shown in Fig. 3 before time t_e.

3. Perform model aggregation, calculate all parameters of each equivalent generator, and calculate the admittance matrix of the equivalent system in box 2 as shown in Fig. 3.

4. Perform transient stability of numerical integration using the equivalent system from t_c.

5. Output the calculation result.

3 Fast emergency control strategy algorithm based on integral sensitivity

All kinds of emergency control algorithms can be described as an optimal control problem that aims at minimizing certain control costs while regarding
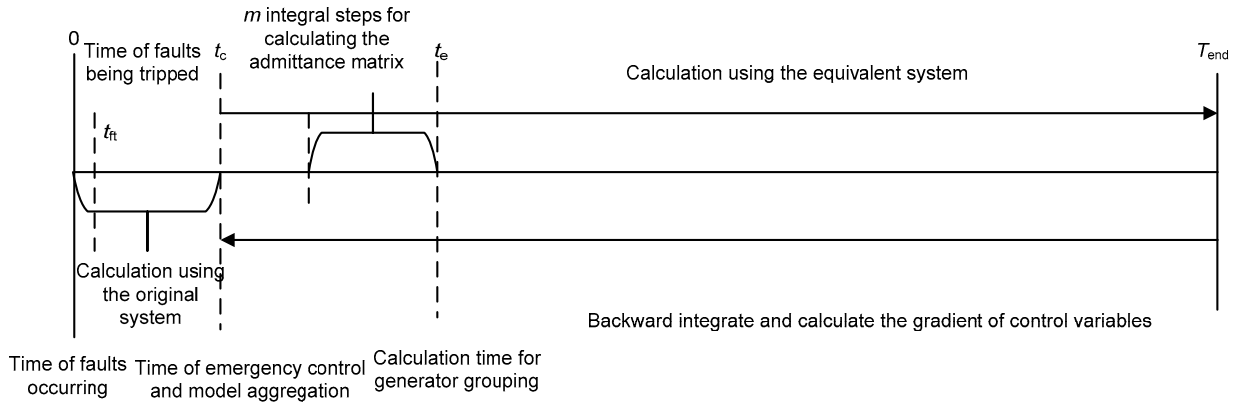
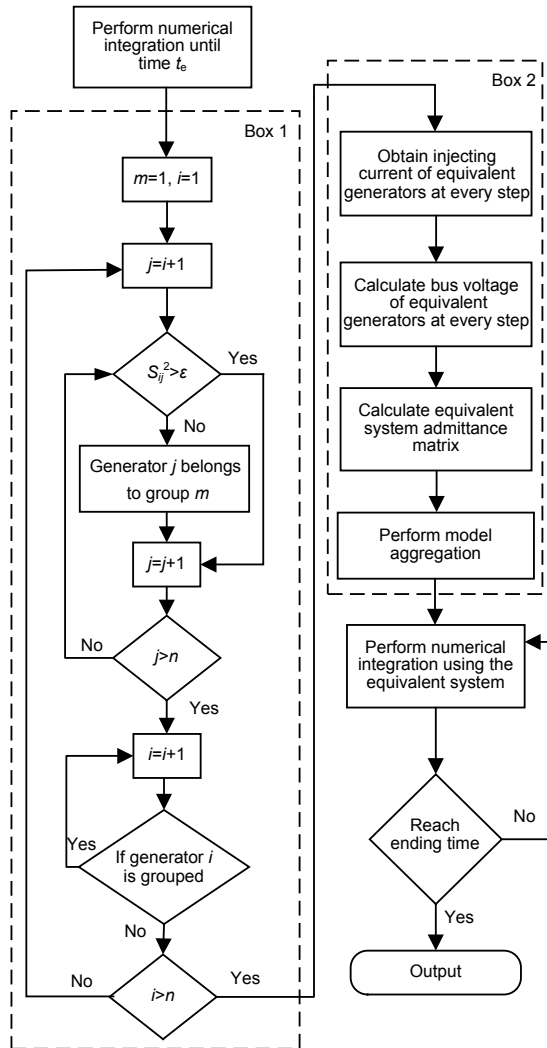**Fig. 2 Timing points and calculation processes**

Fig. 3 Procedure of fast transient stability calculation based on real-time dynamic equivalence

security and stability as constraints. Using the method of integral sensitivity, the control sensitivity of the transient stability constraint function is calculated and the emergency control strategy is obtained for the equivalent system.

3.1 Description of the fast emergency control problem on the equivalent system

As transient stability calculation using the equivalent system substantially reduces the calculation time, in this subsection we will describe how to obtain the emergency control strategy using the equivalent system, which is later reversely mapped to the original system to obtain the final emergency control strategy.

The mathematical model of fast emergency control with transient stability as a constraint that aims at tripping the least number of generators and loads can be described as follows:

Given end time T_{end}, the optimum control u is to minimize the following objective function:

$$J = \sum_{i=1}^{m} c_{\text{G}i} s_{\text{G}i} u_{\text{G}i} + \sum_{j=1}^{m} c_{\text{L}j} s_{\text{L}j} u_{\text{L}j} = \sum_{k=1}^{2m} c_k s_k u_k, \quad (13)$$

where m is the number of equivalent generators, c_k ($k=1, 2, \ldots, 2m$) the weight of each control variable, s_k the single-stage capacity of each control variable, and u_k the control variable.

At the same time, the transient stability constraint should satisfy

$$\theta(u)= \pi^2 - \max\left\{\left[\delta_i(T_{\text{end}}\,|\,u)-\delta_j(T_{\text{end}}\,|\,u)\right]^2\right\}\geq 0, \quad (14)$$

where u_{Gi} is the generator-tripping variable for bus i, u_{Lj} the load shedding variable for bus j, and $\delta_i(T_{\text{end}}|u)$ the rotor angle of generator i at time T_{end} when the control variable is u. $\theta(u)\geq 0$ means that the maximum relative swing angle of the generator rotors is not more than 180° at time T_{end}, which reflects the constraint of transient stability.

3.2 Differential and algebraic equations

According to the classical model of power system analysis, the rotor equation of generator i when the damping coefficient is neglected can be described as

$$\begin{cases} \dfrac{d\delta_i}{dt} = (\omega_i - 1)\omega_s, \\ M_i\dfrac{d\omega_i}{dt} = \dfrac{P_{mi} - P_{ei}}{\omega_i}, \end{cases} \quad i = 1,2,\ldots,m, \quad (15)$$

where $\omega_s = 2\pi f_N$ is the rated electric angular velocity, M_i the inertia constant, P_{mi} the input mechanical power, and P_{ei} the output electrical power.

Assuming that u_{Gi} generators are tripped at bus i, parameters of the remaining generators can be expressed as

$$\begin{cases} M_{si}(P_{msi}) = \dfrac{n_{Gi} - u_{Gi}}{n_{Gi}}M_i(P_{mi}), \\ R_{asi}(X'_{dsi}) = \dfrac{n_{Gi}}{n_{Gi} - u_{Gi}}R_{ai}(X'_{di}), \end{cases} \quad (16)$$

where M_{si}, R_{asi}, X'_{dsi}, P_{msi} and M_i, R_{ai}, X'_{di}, P_{mi} represent the inertia time constant, winding impedance, direct-axis transient reactance, and mechanical power, after and before generator tripping, respectively. n_{Gi} is the total number of generators at bus i.

It can be seen that the state equation does not explicitly contain the generator-tripping control variable u_{Gi} when Eq. (16) is substituted into Eq. (15). However, the generator dummy admittance Y_{dsi} explicitly contains u_{Gi}:

$$Y_{dsi} = \frac{1}{R_{asi} + jX'_{dsi}} = \frac{n_{Gi} - u_{Gi}}{n_{Gi}}\frac{1}{R_{ai} + jX'_{di}}. \quad (17)$$

When laying out the networking equation, the generator dummy admittance should be incorporated into the admittance matrix. Then, the network equation explicitly contains the generator-tripping control variable.

On the other hand, the admittance matrix calculated by the method proposed in Section 2 already includes the constant impedance load in the diagonal elements. The transmission line and constant impedance load parts can be separated according to the basic law of the admittance matrix.

After the equivalent generators and loads are handled, the network equation can be expressed as

$$\begin{bmatrix} \begin{bmatrix} -B_{11} & G_{11} \\ G_{11} & B_{11} \end{bmatrix} & \cdots & \begin{bmatrix} -B_{1m} & G_{1m} \\ G_{1m} & B_{1m} \end{bmatrix} \\ \vdots & & \vdots \\ \begin{bmatrix} -B_{m1} & G_{m1} \\ G_{m1} & B_{m1} \end{bmatrix} & \cdots & \begin{bmatrix} -B_{mm} & G_{mm} \\ G_{mm} & B_{mm} \end{bmatrix} \end{bmatrix}\begin{bmatrix} \begin{bmatrix} V_{y1} \\ V_{x1} \end{bmatrix} \\ \vdots \\ \begin{bmatrix} V_{ym} \\ V_{xm} \end{bmatrix} \end{bmatrix} - \begin{bmatrix} \begin{bmatrix} I'_{x1} \\ I'_{y1} \end{bmatrix} \\ \vdots \\ \begin{bmatrix} I'_{xm} \\ I'_{ym} \end{bmatrix} \end{bmatrix} = \mathbf{0}, \quad (18)$$

where G_{ii} and B_{ii} ($i=1, 2, \ldots, m$) can be expressed as

$$\begin{cases} G_{ii} = G'_{ii} + \dfrac{n_{Li} - u_{Li}}{n_{Li}}G_{Li} + \dfrac{n_{Gi} - u_{Gi}}{n_{Gi}}\dfrac{R_{ai}}{R_{ai}^2 + X'^2_{di}}, \\ B_{ii} = B'_{ii} + \dfrac{n_{Li} - u_{Li}}{n_{Li}}B_{Li} - \dfrac{n_{Gi} - u_{Gi}}{n_{Gi}}\dfrac{X'_{di}}{R_{ai}^2 + X'^2_{di}}, \end{cases} \quad (19)$$

where $G'_{ii} + jB'_{ii}$ represents self-admittance before the generator dummy admittance and the load admittance are merged into the equivalent network, and $G_{Li}+jB_{Li}$ represents the admittance of the equivalent load at bus i.

3.3 Gradient of the objective and constraint functions

It can be seen from Eq. (13) that J does not have any state variable and explicitly contains control variable u, so

$$\nabla J = \left[\frac{\partial J}{\partial u_1},\ldots,\frac{\partial J}{\partial u_{2m}}\right]^T = [c_1s_1,\ldots,c_{2m}s_{2m}]^T. \quad (20)$$

Referring to the problem of optimal emergency control, the gradient of constraint function $\theta(u)$ is expressed as

$$\nabla \theta(u) = \frac{\partial \theta(u)}{\partial u}$$
$$= \int_{t_c}^{T_{end}} \frac{\partial H[x(t \mid u), y(t \mid u), u, \lambda(t \mid u), \beta(t \mid u)]}{\partial u} \mathrm{d}t, \quad (21)$$

where $H(x, y, u, \lambda, \beta)$ is the Hamiltonian function of constraint function $\theta(u)$ and t_c is the time of generator tripping or load shedding. T_{end} is the total simulation time.

$$H(x, y, u, \lambda, \beta) = \lambda^{\mathrm{T}} g(x, y, u) + \beta^{\mathrm{T}} \Phi(x, y, u)$$
$$= \sum_{i=1}^{m} [\lambda_{i1}, \ \lambda_{i2}] \begin{bmatrix} (\omega_i - 1)\omega_s \\ \frac{1}{M_{Ji}}(P_{mi} - P_{ei}) \end{bmatrix},$$
$$+ \sum_{i=1}^{m} [\beta_{i1}, \ \beta_{i2}] \begin{bmatrix} \sum_{j=1}^{m} (-B_{ij}U_{jy} + G_{ij}U_{jx}) - I'_{xi} \\ \sum_{j=1}^{m} (G_{ij}U_{jy} + B_{ij}U_{jx}) - I'_{yi} \end{bmatrix}. \quad (22)$$

$\lambda(t \mid u) \in \mathbb{R}^{2m}$ and $\beta(t \mid u) \in \mathbb{R}^{2m}$ are solutions of the co-state differential algebraic equations, expressed as

$$\lambda = -\frac{\partial H[x(t \mid u), y(t \mid u), u, \lambda(t \mid u), \beta(t \mid u)]}{\partial x}, \quad (23)$$

$$\lambda(T_{end}) = \frac{\partial \theta(u)}{\partial x}, \quad (24)$$

$$0 = \frac{\partial H[x(t \mid u), y(t \mid u), u, \lambda(t \mid u), \beta(t \mid u)]}{\partial y}. \quad (25)$$

The calculation procedure for the transient stability constraint function gradient (Algorithm 2) is summarized below:

1. Execute transient stability calculation during time interval $(t_c, T_{end}]$ with u being given and obtain $x(t \mid u)$ and $y(t \mid u)$.

2. Solve the co-state equation using reverse numerical integration during time interval (t_c, T_{end}).

3. Solve the gradient according to Eq. (21). Because the numerical method is adopted in Eqs. (23)–(25), the integration of Eq. (21) is converted into summation operations.

3.4 Control sensitivity

Using Eq. (21), we obtain the gradient of the transient stability constraint function for each control variable, which can be regarded as the improvement of stability after tripping a single-stage generator or shedding a single-stage load. The gradient for a certain control variable is proportional to its single-stage capacity. Dividing each gradient by its corresponding single-stage capacity S_i, the obtained value K_i is relevant only to the location of the control variable, which is called "control sensitivity":

$$K_i = \frac{1}{s_i} \frac{\partial \theta}{\partial u_i}. \quad (26)$$

The control sensitivity values will be used to select the best control location.

4 Reverse mapping of the emergency control strategy

Only the emergency control strategy for the equivalent system can be obtained using Algorithms 1 and 2, and this should be reverse mapped to the original system. The link between the control variable of the equivalent system and the original system is the relevant capacity of the generators and loads. Reverse mapping can be performed only when the specific power supply situation from each generator to each load is obtained.

4.1 Positive sequential power flow tracing

The method traces power flow from generators to loads (Abdelkader, 2007; Rao et al., 2010; Zhu et al., 2016). The power supply percentage of load k from generator i is

$$\mathrm{up}_{Lk}^{Gi} = \frac{\left[A_d^{-1}\right]_{ik} p_{Lk}}{p_i}, \quad (27)$$

where P_{Lk} is the actual power of load k, P_i the total outgoing line power flow from bus i, and $[A_d]_{ik}$ the allocation matrix, expressed as

$$[A_d]_{il} = \begin{cases} 1, & i = l, \\ -\dfrac{|p_{l-i}|}{p_l}, & l \in \alpha_i^{(d)}, \\ 0, & \text{otherwise}, \end{cases} \quad (28)$$

where $\alpha_i^{(d)}$ is the outgoing line set of bus i and p_{l-i} is $l-i$ branch power flow drawn from bus i.

4.2 Reverse mapping of the control strategy

Algorithm 1 clearly indicates which generator belongs to a certain equivalent generator. For example, the generator set of the equivalent generator i is $\{G_{i1}, G_{i2}, \ldots, G_{ing}\}$. If u_{Gi} stages of the equivalent generator i are tripped, generators of the same total capacity in this set should also be tripped in the original system.

The equivalent system clusters large numbers of loads and a certain generator in one equivalent bus. In principle, if some loads draw power flow from a certain generator, then they are aggregated. When u_{Li} stages of loads are shed at equivalent bus i, the generator set $\{G_{i1}, G_{i2}\ldots, G_{ing}\}$ and the load set of each generator G_{ik} are obtained using power flow tracing. Then, a total load set $\{L_{i1}, L_{i2}, \ldots, L_{inl}\}$ related to equivalent bus i can be obtained. The number of stages of load L_{ip} that should be shed is determined by

$$u_{L_{ip}} = \sum_{k=1, L_{ip} \in G_{ik}}^{ng} \mathrm{up}_{L_{ip}}^{G_{ik}} \cdot u_{Li}. \qquad (29)$$

5 Procedure of the fast emergency control strategy algorithm based on real-time dynamic equivalence and integral sensitivity

The emergency control strategy algorithm should be carefully designed because the sensitivity of the control variable constantly changes over time. First, a method of discontinuously updating sensitivity is adopted. A counter n is defined in the calculation process, which increases by one when a control variable is corrected. The sensitivity of each control variable should be updated when $n>n_{max}$, where n_{max} is the threshold of sensitivity updating and generally it is set at three or four. Second, the characteristics of different control variables are not the same. For instance, the change of sensitivity after load shedding is much smaller than that of generator tripping. If the control measurement contains only load shedding, the original sensitivity can be corrected only by Eq. (30). However, the sensitivity of each control variable should be recalculated as long as the control measurement contains generator tripping. When the control variables have changed, the generators' power

angles may present different dynamic responses and the primary grouping result is no longer suitable for the new control variables. In other words, numerical integration using the original system from time t_c to t_e, generator grouping, model aggregation, and the admittance matrix is recalculated if the sensitivity should be recalculated. In Section 6.2, the actual computation time cost by this process will be further analyzed, and it will be shown that this process takes little time, although it should be done whenever the sensitivity needs to be recalculated.

Algorithm 3:

1. Read system data and run power flow.

2. Perform the dynamic equivalence and transient stability calculation according to Algorithm 1. The algorithm ends if the system is stable after disturbance; otherwise, proceed to the next step.

3. Calculate the control gradient of the transient stability constraint function using the equivalent system according to Algorithm 2, calculate the control sensitivity, and set counter $n=0$.

4. Sort all control sensitivities in descending order.

5. Increase a control variable according to

$$K_i S_i \Delta u_i + \theta(u) = 0, \ \ \Delta u_i = [\Delta u_i] + 1, \qquad (30)$$

where [ ] means the maximum integer that is no larger than the inside number.

If $\Delta u_i > r_i$, set $\Delta u_i = r_i$, where r_i is the maximum permitted value of generator-tripping stages or load shedding stages for control variable i.

6. Set $n=n+1$. If the control variable contains a generator of $K_i S_i \Delta u_i + \theta(u) > 0$ or $n > n_{max}$, go to step 7; otherwise, update $\theta(u) = \theta(u) + K_i S_i \Delta u_i$, go back to step 5, and calculate the next control variable according to the descending order in step 4.

7. Set $n=0$. Map the control strategy to the original system. Reserve the new control strategy for the original system, and perform numerical integration using the original system from time t_c to t_e. Perform generator grouping and model aggregation, and recalculate the admittance matrix. Perform forward integration from time t_c to T_{end} using the equivalent system to obtain the new value of the constraint function and calculate the new control sensitivities. Go to step 8 if the system is stable; otherwise, go to step 4.

8. Decrease the control variable in ascending order of sensitivity among nonzero control variables until the system loses stability, and go to step 9.

9. Successively decrease the control variable among nonzero control variables until the system loses stability.

10. Map the emergency control strategy to the original system and obtain the final strategy. If the original system regains transient stability, the whole algorithm ends; otherwise, recalculate the strategy according to steps 2–9, reserving the existing strategy for another time.

Steps 8 and 9 are to ensure that the algorithm avoids unnecessary generator tripping and load shedding. Decrease the control variable and perform forward integration only as in step 7 to see if the system is stable. If so, the new control variable is adopted; otherwise, reserve the original control variable. These two steps do not include backward integration or calculation of sensitivity.

6 Simulation results

6.1 Fast transient stability calculation based on real-time dynamic equivalence

Simulations were performed on the East China Power System that contains 496 generators and 5075 buses using the method proposed in this study. The integration step length was 0.01 s. The total simulation time T_{end} was 3 s, and time t_e was set at 0.6 s.

Case 1 A three-phase short circuit occurred at bus 4044 on the East China Power System and the line from bus 4041 to bus 4044 was removed after 0.1 s. Rotor angles calculated by conventional numerical integration are shown in Fig. 4.

The 496 generators were divided into five groups at 0.6 s. Numerical integration was performed using the equivalent system. The rotor angle curves are shown in Fig. 5.
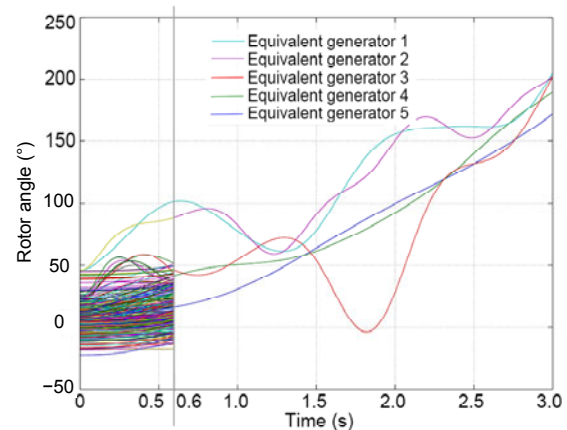
Comparing Figs. 4 and 5, after generator model aggregation and admittance matrix calculation, the accurate rotor angle curves of the five equivalent generators were obtained. The maximum rotor angle difference obtained was the same as that before equivalence.

Case 2 A three-phase short circuit occurred at bus 3950 and the line from bus 3950 to bus 2908 was removed after 0.1 s. The rotor angles calculated by numerical integration are shown in Fig. 6.
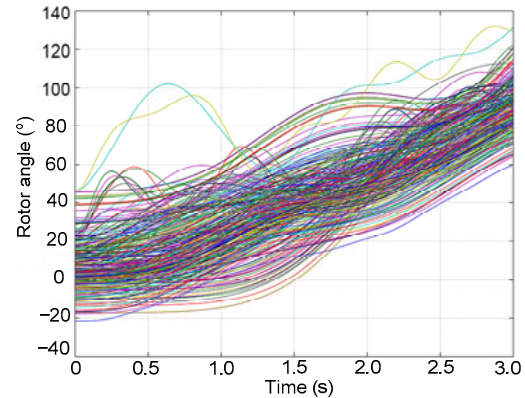
Fig. 4 Rotor angles computed by the conventional numerical integration algorithm (References to color refer to the online version of this figure)

Fig. 5 Rotor angles computed by the proposed algorithm in case 1 (References to color refer to the online version of this figure)
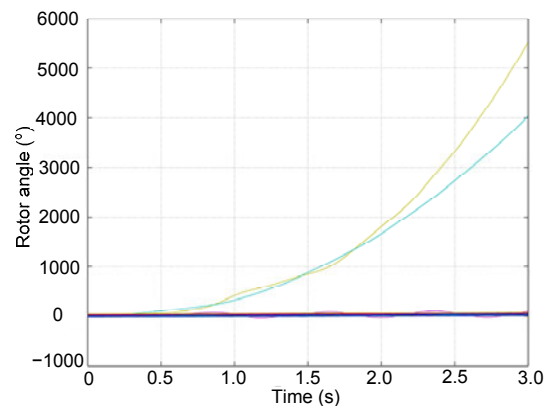
Fig. 6 Rotor angles computed by the numerical integration algorithm (References to color refer to the online version of this figure)
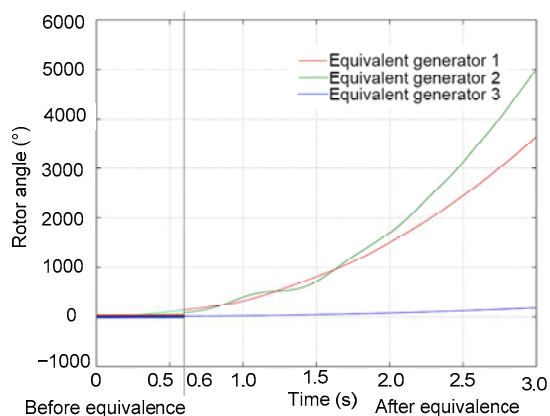
The 496 generators were divided into three groups. Power angles calculated by numerical integration using the equivalent system are shown in Fig. 7.

Fig. 7 Rotor angles computed by the proposed algorithm in case 2 (References to color refer to the online version of this figure)

Comparing Figs. 6 and 7, after generator model aggregation and admittance matrix calculation, accurate rotor angles of the three equivalent generators were obtained. The maximum angle difference obtained was the same as that before equivalence.

There were 100 faults tested on the East China Power System. In all these tests, it was found that the number of generator groups seldom exceeded 10, which led to a great reduction in calculation time. The proposed algorithm can obtain the accurate maximum rotor angle difference, with an error that did not exceed 10%. This algorithm saved more than 60% of the calculation time on the East China Power System, demonstrating its potential for real-time applications.

Some detailed calculation results on the East China Power System are shown in Table 1 (Intel® Core™ i3-2100 CPU@3.10 GHz was used in the simulations).

6.2 Fast emergency control strategy algorithm based on real-time dynamic equivalence and integral sensitivity

Emergency control was employed on an unstable case in Section 6.1 using Algorithm 3. Considering that the typical power plant contained four or so generators and a transformer substation contained 8–10 lines, the number of generator-tripping stages was set at four and that of the load shedding stages was set at eight. Emergency control acted at time t_c=0.3 s and numerical integration using the original system was calculated when t_e=0.6 s. In the simulation, if the maximum rotor angle difference was less than 180°, the system was identified as stable.

Case 3   The calculation of the emergency control strategy for case 2 was given here in detail. For process 1 in Table 2, transient stability calculation was performed in case 2 and all control sensitivities can be calculated by Algorithm 2, the largest of which was generator-tripping control at bus 3. The generator-tripping strategy of bus 3 consisted of two stages according to Eq. (30), and it was found that generator 228 in the original system was connected to bus 3 in the equivalent system. Because generator tripping was concerned, the sensitivities should be recalculated. For process 2 in Table 2, numerical integration was recalculated using the original system from time t_c to t_e. Generators were grouped again and the result for grouping remained unchanged. The model aggregation and admittance matrix were recalculated. Numerical integration was performed using the equivalent system and the system was still unstable. The control sensitivities were recalculated, and the largest control sensitivity was the generator-tripping control at bus 2. Then, according to Eq. (30), the generator-tripping strategy consisted of two stages at bus 2 and generator 223 in the original system was connected to bus 2 in the equivalent system. Because

Table 1 Results of some calculations on the East China Power System

Case	Maximum rotor angle difference (°)		Error (%)	Number of groups	Calculation time (ms)		Time saved (%)
	Conventional algorithm	Algorithm 1			Conventional algorithm	Algorithm 1	
1	5312.57	4897.900	7.81	3	852.88	188.08	77.95
2	440.12	473.481	7.58	3	903.22	270.51	70.05
3	538.74	495.856	7.96	2	783.24	193.34	75.32
4	300.52	321.737	7.06	4	882.36	255.44	71.05
5	9166.00	9755.374	6.43	2	832.45	182.56	77.95

Table 2 Calculation time for the seven processes in Algorithm 3

Stage	Calculation time (s)						
	1	2	3	4	5	6	7
Numerical integration using the original system time from 0 to t_c	0.0826	–	–	–	–	–	–
Numerical integration using the original system time from t_c to t_e	0.0883	0.0964	0.0923	0.0943	0.0978	0.0911	0.0989
Generator grouping	0.0079	0.0077	0.0073	0.0065	0.0067	0.0053	0.0070
Model aggregation	0.0052	0.0059	0.0063	0.0064	0.0052	0.0064	0.0060
Admittance matrix calculation	0.0349	0.0419	0.0427	0.0417	0.0408	0.0451	0.0431
Forward integration using the equivalent system time from t_c to T_{end}	0.0036	0.0048	0.0040	0.0043	0.0038	0.0034	0.0040
Backward integration using the equivalent system time from T_{end} to t_c	0.0048	0.0061	0.0055	–	–	–	–
Reserve mapping	0	0	0	0	0	0	0
Numerical integration using the original system time from t_c to T_{end}	–	–	–	–	–	–	0.8066

generator tripping was involved, the sensitivities should be recalculated. For process 3 in Table 2, the same processes were completed for the new control strategy. The system was stable and the new sensitivities were calculated. For process 4 in Table 2, corresponding to step 8, generator tripping was decreased by one stage for generator 228; however, the system was unstable. For processes 5 and 6 in Table 2, generator tripping was decreased by one stage for generator 223 and the system remained stable; however, the system was unstable if generator tripping was deceased by two stages. For process 7 in Table 2, corresponding to step 9, generator tripping was again decreased by one stage for generator 228; however, the system was unstable. So, the final control strategy was two stages of generator tripping for generator 228 (bus 830) and one stage of generator tripping for generator 223 (bus 824). The maximum rotor angle at the end of the calculation was 69.64°. The time used for calculation was 2.13 s.

To show the effectiveness and high efficiency of the proposed algorithm, a conventional algorithm was applied as a comparison. The conventional algorithm used the same method of numerical integration and sensitivity calculation.

For case 2, the calculation process of the emergency control strategy using the conventional algorithm is shown in Table 3. Transient stability calculation was performed and all control sensitivities were calculated, the largest of which was the generator-tripping control for generator 228. The generator-

tripping strategy consisted of four stages according to Eq. (30). Numerical integration was recalculated from time t_c and the system was stable. Corresponding to step 9, generator tripping was decreased by one stage for generator 228 and the system was still stable. Then, generator tripping was decreased by one stage for generator 228; however, the system was unstable. Therefore, the final control strategy was three stages of generator tripping for generator 228 (bus 830). The maximum rotor angle at the end of the calculation was 97.11°. The time used for calculation was 4.05 s.

By comparing the two algorithms, the most remarkable difference was that Algorithm 3 transferred forward and backward integration between time t_c and T_{end} from the original system to the equivalent system. Although the sensitivities may be calculated more times, the calculation time for each one and the whole calculation time were substantially decreased, which can be noticed from the detailed calculation time for each process in Tables 2 and 3.

Corresponding to Table 1, detailed simulation results of emergency control are shown in Table 4. From Table 4, it can be seen that the control strategy calculated by Algorithm 3 may not be completely consistent with that obtained by the conventional method. If an equivalent load was shed, the relevant loads in the original system were shed in the proportion calculated by power flow tracing; however, some of these loads should be shed only if the conventional algorithm was applied. Although the number of loads that should be shed may decrease, the capacity shed in

Table 3 Calculation time for the four processes using the conventional algorithm

Process time	Calculation time (s)			
	1	2	3	4
Numerical integration time from 0 to t_c	0.0897	–	–	–
Forward integration time from t_c to T_{end}	0.7812	0.7837	0.7936	0.7901
Backward integration time from T_{end} to t_c	0.7879	–	–	–

Table 4 Calculation results using the emergency control strategy

Fault set		Maximum power angle (°)		Control strategy		Calculation time (s)		Time saved (%)
Bus	Line	Before control	After control	Conventional algorithm	Algorithm 3	Conventional algorithm	Algorithm 3	
3950	2508–3950	5312.57	69.64	Three stages of generators being tripped at bus 830 (262.5 MW)	One stage of generators being tripped at bus 824; two stages of generators being tripped at bus 830 (207.5 MW)	4.0479	2.1306	47.37
4620	4322–4620	440.12	75.70	Two stages of generators being tripped at bus 734; two stages of generators being tripped at bus 736 (16 MW)	Seven stages of loads being shed at bus 3101 (12.19 MW); one stage of generators being tripped at bus 736 (6.25 MW)	25.3271	3.9754	84.30
4634	4469–4634	538.74	156.69	Three stages of generators being tripped at bus 736 (56.25 MW)	Three stages of generators being tripped at bus 736 (56.25 MW)	14.4940	2.1179	85.39
4323	2691–4323	300.52	84.30	Eight stages of loads shed at bus 735; eight stages of loads shed at bus 736; eight stages of loads being shed at bus 740 (11.16 MW)	Eight stages of loads being shed at bus 735; eight stages of loads being shed at bus 738; eight stages of loads being shed at bus 739; two stages of loads being shed at bus 741 (6.74 MW)	7.1310	1.9148	73.15
810	810–3430	9166.00	68.33	Four stages of generators being tripped at bus 804; four stages of generators being tripped at bus 805; four stages of generators being tripped at bus 807; four stages of generators being tripped at bus 808 (110 MW)	Four stages of generators being tripped at bus 804; four stages of generators being tripped at bus 805; four stages of generators being tripped at bus 807; four stages of generators being tripped at bus 808; (110 MW)	15.2795	2.8742	81.19

The bus column represents the buses, in which the three-phase short circuit fault occurs; the line column represents the lines that are removed 0.1 s after the fault

each load increased in the interim. So, the total capacity of loads shed in different systems did not appear to be much different, although the allocation proportion between loads may be different.

The active power values for generator tripping and load shedding are given in Table 4. Actually, there was no need to obtain a much smaller actual power for

generator tripping or load shedding compared with the conventional algorithm. However, the algorithm should make sure that the strategy obtained is effective and that the amount of generator tripping and load shedding is the same as or smaller than that calculated by the conventional algorithm. Also, the algorithm itself should avoid unnecessary generator

tripping or load shedding, which is ensured by steps 8 and 9 in Algorithm 3.

It was found that the final emergency strategy obtained in Algorithm 3 was highly effective with less computation and difficulty. Since the algorithm aimed to realize online applications, power systems of different scales were tested using the proposed algorithm. For instance, the algorithm was also applied to some smaller power systems in simulations, and the calculation results of the emergency control strategy for the IEEE39 system are given in Table 5. It can be found that, at the present stage, the algorithm has the potential to be used in online pre-decision. Since the algorithm substantially decreases the calculation time, for a given operation condition and contingency set, it could rapidly calculate the control strategy for the contingency and update the strategy table. On the other hand, more efforts should be made for the algorithm, for instance, parallel computing, which could be further researched to finally realize real-time emergency control.

7 Conclusions

In this paper, the whole procedure for a new emergency control algorithm based on real-time dynamic equivalence and integral sensitivity has been proposed, in which a new transient stability simulation algorithm has been used. A fast calculation method for the equivalent system admittance matrix has been proposed. The algorithm not only has high precision, good convergence, and good adaptability, but also greatly simplifies the calculation. The results are expected to realize online fast transient stability analysis and fast emergency control. Based on this work, we will continue to research the following:

1. Expand the generator models and verify the algorithm on more detailed generator models, using the generators with an exciter and a governor and the loads with an induction motor.

2. Apply the proposed algorithm to transient stability preventive control and develop an accurate preventive control strategy scheme.

3. Further investigate how the proposed method is suitable for parallel computing and how the concrete process for parallel computing is realized.

Compliance with ethics guidelines

References

Abdelkader SM, 2007. Transmission loss allocation through complex power flow tracing. *IEEE Trans Power Syst*, 22(4):2240-2248.
https://doi.org/10.1109/TPWRS.2007.907586

Chiang HD, 2011. Direct Methods for Stability Analysis of Electric Power Systems: Theoretical Foundation, BCU Methodologies, and Applications. John Wiley & Sons, New York, USA.

Table 5 Calculation results of the emergency control strategy for the IEEE39 system

Fault set		Maximum power angle (°)		Control strategy	Calculation time (ms)
Bus	Line	Before control	After control		
10	10–32	7497.27	34.41	Four stages of generators being tripped at bus 32	58.07
19	19, 20	1793.92	26.82	One stage of generators being tripped at bus 33; two stages of loads being shed at bus 20	62.19
16	16–19	3410.26	87.46	Two stages of generators being tripped at bus 33; two stages of generators being tripped at bus 34	34.20
20	19, 20	1705.44	107.64	Two stages of loads being shed at bus 20	43.98
37	25–37	9204.60	26.71	Four stages of generators being tripped at bus 37	55.13
29	26–29	5009.22	59.62	Two stages of generators being tripped at bus 38	28.58
6	6–31	7694.25	31.95	Four stages of generators being tripped at bus 31	70.82
36	23–36	8765.41	35.23	Four stages of generators being tripped at bus 36	35.31
35	22–35	7732.51	34.85	Four stages of generators being tripped at bus 35	26.75
20	20–34	7942.93	34.62	Four stages of generators being tripped at bus 34	51.44

Euxibie E, Goubin M, Heilbronn B, et al., 1992. Prospects of application to the French system of fast methods for transient stability and voltage security assessment. Proc CIGRE Conf, p.38-208.

Jiang QY, Wang Y, Geng GC, 2014. A parallel reduced-space interior point method with orthogonal collocation for first-swing stability constrained emergency control. *IEEE Trans Power Syst*, 29(1):84-92. https://doi.org/10.1109/TPWRS.2013.2275175

Li YQ, Tenglin, Liu WS, et al., 2002. The study on real-time transient stability emergency control in power system. Proc IEEE Canadian Conf on Electrical and Computer Engineering, p.138-143. https://doi.org/10.1109/CCECE.2002.1015188

Nakawiro W, Erlich I, 2009. Optimal load shedding for voltage stability enhancement by ant colony optimization. Proc 15th Int Conf on Intelligent System Applications to Power Systems, p.1-6. https://doi.org/10.1109/ISAP.2009.5352886

Rao MSS, Soman SA, Chitkara P, et al., 2010. Min-max fair power flow tracing for transmission system usage cost allocation: a large system perspective. *IEEE Trans Power Syst*, 25(3):1457-1468. https://doi.org/10.1109/TPWRS.2010.2040638

Song H, Kezunovic M, 2004. Stability control using PEBS method and analytical sensitivity of the transient energy margin. Proc IEEE Power Systems Conf and Exposition, p.1153-1158. https://doi.org/10.1109/PSCE.2004.1397700

Tian F, Zhang X, Yu ZH, et al., 2016. Online decision-making and control of power system stability based on super-real-time simulation. *CSEE J Power Energy Syst*, 2(1):95-103. https://doi.org/10.17775/CSEEJPES.2016.00014

Wang XF, Song Y, Irving M, 2008. Modern Power System Analysis. Springer, New York, USA. https://doi.org/10.1007/978-0-387-72853-7

Xue Y, 1993. An emergency control framework for transient security of large power systems. Int Symp on Power Systems, p.120-125.

Xue Y, Pavella M, 1989. Extended equal-area criterion: an analytical ultra-fast method for transient stability assessment and preventive control of power systems. *Int J Electr Power Energy Syst*, 11(2):131-149. https://doi.org/10.1016/0142-0615(89)90021-5

Xue Y, van Cutsem T, Ribbens-Pavella M, 1988a. A simple direct method for fast transient stability assessment of large power systems. *IEEE Trans Power Syst*, 3(2):400-412. https://doi.org/10.1109/59.192890

Xue Y, van Cutsem T, Ribbens-Pavella M, 1988b. Real-time analytic sensitivity method for transient security assessment and preventive control. *IEE Proc C-Gener Trans Distrib*, 135(2):107-117. https://doi.org/10.1049/ip-c.1988.0013

Xue Y, Wehenkel L, Belhomme R, et al., 1992. Extended equal area criterion revisited (EHV power systems). *IEEE Trans Power Syst*, 7(3):1012-1022. https://doi.org/10.1109/59.207314

Xue Y, Luo Y, Xue F, et al., 1993. On-line transient stability assessment in operation—DEEAC in Northeast China Power System. Proc IEEE Region 10th Int Conf on Computers, Communications and Automation, p.72-76. https://doi.org/10.1109/TENCON.1993.320588

Xue YS, Zhang YW, 1990. Direct transient stability assessment with two-axis generator models. *IFAC Proc Vol*, 23(8):7-12. https://doi.org/10.1016/S1474-6670(17)51390-7

Yuan Y, Kubokawa J, Sasaki H, 2003. A solution of optimal power flow with multicontingency transient stability constraints. *IEEE Trans Power Syst*, 18(3):1094-1102. https://doi.org/10.1109/TPWRS.2003.814856

Zhu SM, Wu L, Guan XH, et al., 2016. SCUC-based optimal power tracing approach for scheduling physical bilateral transactions and its verification via an integrated power-money flow analysis. *IET Gener Trans Distrib* 10(10):2399-2409. https://doi.org/10.1049/iet-gtd.2015.1160